crystals

MDPI

Article

Textile Functionalization by Porous Protein Crystal Conjugation and Guest Molecule Loading

Luke F. Hartje [1,†], David A. Andales [2,†], Lucas P. Gintner [2], Lucas B. Johnson [2], Yan V. Li [3] and Christopher D. Snow [1,2,*]

[1] Department of Biochemistry and Molecular Biology, Colorado State University, Fort Collins, CO 80523, USA
[2] Department of Chemical and Biological Engineering, Colorado State University, Fort Collins, CO 80523, USA
[3] Department of Design and Merchandizing, Colorado State University, Fort Collins, CO 80523, USA
* Correspondence: christopher.snow@colostate.edu
† These authors contributed equally to this work.

Abstract: Protein crystals are versatile nanostructured materials that can be readily engineered for applications in nanomedicine and nanobiotechnology. Despite their versatility, the small size of typical individual protein crystals (less than one cubic mm) presents challenges for macroscale applications. One way to overcome this limitation is by immobilizing protein crystals onto larger substrates. Cotton is composed primarily of cellulose, the most common natural fiber in the world, and is routinely used in numerous material applications including textiles, explosives, paper, and bookbinding. Here, two types of protein crystals were conjugated to the cellulosic substrate of cotton fabric using a 1,1′-carbonyldiimidazole/aldehyde mediated coupling protocol. The efficacy of this attachment was assessed via accelerated laundering and quantified by fluorescence imaging. The ability to load guest molecules of varying sizes into the scaffold structure of the conjugated protein crystals was also assessed. This work demonstrates the potential to create multifunctional textiles by incorporating diverse protein crystal scaffolds that can be infused with a multiplicity of useful guest molecules. Cargo molecule loading and release kinetics will depend on the size of the guest molecules as well as the protein crystal solvent channel geometry. Here, we demonstrate the loading of a small molecule dye into the small pores of hen egg white lysozyme crystals and a model enzyme into the 13-nm pores delimited by "CJ" crystals composed of an isoprenoid-binding protein from *Campylerbacter jejuni*.

Keywords: protein crystals; crosslinking; host–guest crystals; bioconjugation; textile engineering

Citation: Hartje, L.F.; Andales, D.A.; Gintner, L.P.; Johnson, L.B.; Li, Y.V.; Snow, C.D. Textile Functionalization by Porous Protein Crystal Conjugation and Guest Molecule Loading. *Crystals* **2023**, *13*, 352. https://doi.org/10.3390/cryst13020352

Academic Editors: Blaine Mooers and Borislav Angelov

Received: 30 December 2022
Revised: 11 February 2023
Accepted: 15 February 2023
Published: 18 February 2023

1. Introduction

Protein crystal materials are alternative porous scaffolds to traditional non-biological nanoporous materials such as zeolites or metal organic frameworks (MOFs). Efforts to characterize protein crystals have led to advancements in crystal production, stabilization, and design—increasing their appeal for material applications. Protein crystal materials are attractive for many reasons: they are self-assembling, exhibit a highly ordered porous structure, have been shown to be biodegradable and biocompatible [1,2], and can be engineered with relative ease through genetic modification or chemical conjugation. Protein crystal materials have been utilized in a variety of disciplines for various applications ranging from biocatalysis [3–12] and chromatography [13–18] to drug delivery [19–22] and biosensing [23–26]. Here, we propose implementing protein crystals as tunable porous scaffolds for the organization and containment of diverse functional guest molecules in the interest of producing multifunctional textile materials.

A typical protein crystal contains uniform solvent-filled channels ranging from 30 to 60% of the total crystal volume [27]. These pores can be employed as a reservoir for guest molecules of assorted size and functionality including various small molecules,

enzymes, therapeutic proteins, and deoxyribonucleic acid (DNA) as well as nanoparticles and organometallic compounds. Despite their remarkable qualities, the use of protein crystals in conventional macroscale material science applications is limited due to their small size (commonly <1 mm). This limitation may be overcome by devising methods for integrating protein crystals into larger host materials. Textiles are inexpensive and widely used across many industries, making them attractive host materials for protein crystal bioconjugation. By conjugating crystals to textiles, a multifunctional macroscale nanoporous scaffold material can be realized.

We investigated two distinct protein crystal variants, each with dramatically different pore size distributions, geometries, and lumenal environments. The first crystal variant tested was tetragonal hen egg white lysozyme (HEWL), a relatively inexpensive and well-characterized protein (Figure 1A). Cvetkovic et al. determined that the pores of cross-linked tetragonal HEWL crystals accept small molecule guests with an effective diameter below 0.73 ± 0.06 nm [28–30]. Our other protein crystal building block is "CJ", a putative isoprenoid binding protein from *Campylobacter jejuni*, which can grow crystals with unusually large axial pores exceeding 13 nm in diameter. CJ protein crystals, our second crystal variant, are thus a member of the large-pore protein crystal (LPC) class—possessing pores that enable the uptake of macromolecular guests (Figure 1B). Typical CJ derived large-pore protein crystals (CJ-LPCs) possess hundreds of millions of pores and can be engineered with capture sites within the nanopores for the purpose of organizing macromolecular guests at distinct sites [31–34]. The combination of high theoretical capacity for guest molecules and mechanical strength after cross-linking makes porous protein crystals attractive molecular depots for use in multifunctional macroscale nanoporous scaffold materials.

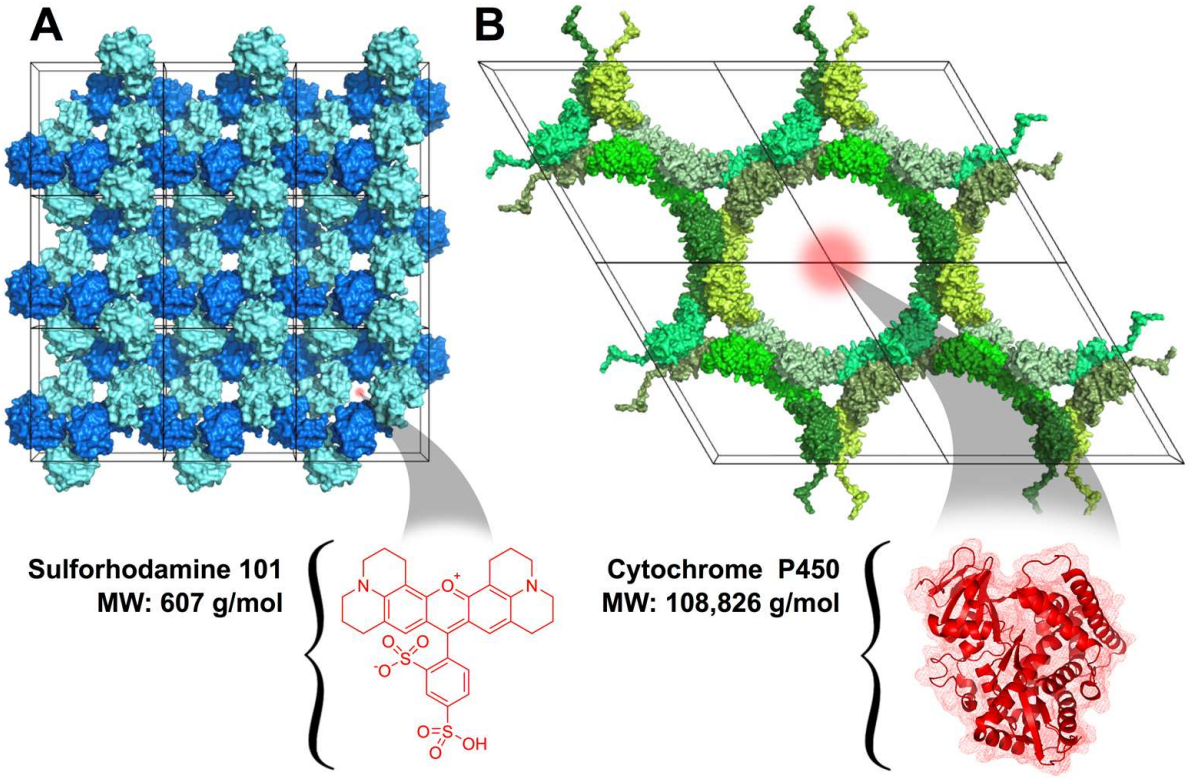

Figure 1. (**A**) Cross-linked tetragonal HEWL crystal lattice (PDB: 2HTX) showing small archetypal protein crystal pore sizes (<2 nm) that can accommodate small molecules such as sulforhodamine 101. (**B**) CJ-LPC crystal lattice (PDB: 5W17) shows much larger (13 nm diameter) pores that can accommodate macromolecular guests such as the cytochrome P450 heme domain (PDB: 2HPD).

2. Materials and Methods

Reagents: The following chemicals were purchased and used without further purification. From Sigma-Aldrich: acetone, 1,1′-carbonyldiimidazole (CDI), dimethylamine borane complex (DMAB), trimethylamine N-oxide (TMAO), glutaraldehyde solution (GA) (25% in H_2O), sodium phosphate dibasic (Na_2HPO_4), sodium hypophosphite monohydrate, potassium phosphate monobasic (KH_2PO_4), and ammonium sulfate ($[NH_4]_2SO_4$). From VWR: HEPES and bis-tris. From Acros Organics: glyoxal (oxaldehyde) solution (40% in H_2O), carbohydrazide. From EMD Millipore: sulfuric acid (H_2SO_4) and sodium acetate. From Tokyo Chemical Industry Co.: adipic acid dihydrazide (AAD). From Fisher Scientific: sodium borate, NHS-fluorescein, sulforhodamine 101 (non-reactive), NaCl, and KCl. From J.T. Baker: citric acid. From Chemodex: sulforhodamine 101 acid chloride (TexasRed). From Hampton Research: lyophilized hen egg white lysozyme (HEWL).

Protein Expression and Purification: The target gene CJ was modified from the gene vector encoding protein CJ0 obtained from the Protein Structure Initiative: Biology-Materials Repository (Genebank ID: cj0420, Protein Data Bank ID: 5w17). For ease of uniform expression and purification, the CJ0 gene was codon optimized and the periplasmic signaling peptide deleted, thereby yielding CJ. The CJ gene was encoded in the expression vector pSB3 with a C-terminal 6xHis tag and expressed in Escherichia coli C41-DE3 cells. A total of 1 mL of turbid starter culture was added to 500 mL Terrific Broth (TB) with 100 mg/mL kanamycin and incubated at 37 °C with shaking at 250 rpm until lightly turbid (~2.5–3 h). Protein expression was induced with 0.4 mM isopropyl β-D-1-thiogalactopyranoside (IPTG) followed by overnight (~16 h) incubation at 25 °C with shaking at 250 rpm. Cells were lysed by sonication and the CJ protein purified via gravity Ni-NTA affinity capture, followed by ammonium sulfate ($[NH_4]_2SO_4$) precipitation. Purified CJ protein was buffer exchanged into 0.5 M $[NH_4]_2SO_4$, 10 mM HEPES, and 10% glycerol at pH 7.4, concentrated to ~40 mg/mL, and stored at −30 °C.

HEWL Batch Crystallization: Three stock solutions were made: 2.74 M NaCl in deionized (DI) water, 85 mg/mL HEWL in DI water, and 100 mM sodium acetate pH 4.6 in DI water. HEWL stock solution was stored at 10 °C or lower when not in use. The three stock solutions were added to a single well of a nine cavity PYREX® spot plate in consecutive order: 50 µL sodium acetate solution, 50 µL NaCl solution, and 100 µL HEWL stock solution. The solution mixture was gently pipetted to mix and allowed to incubate without disturbance at room temperature for 24 h. After 24 h, visible lysozyme crystals could be seen in solution and on the surface of the glass plate; longer growth times yielded larger crystals.

CJ-LPC Batch Crystallization: Approximately 40 mg/mL CJ was mixed with 3.4 M $[NH_4]_2SO_4$, 40 mM bis-tris pH 6.5 in a PYREX® spot plate well at a protein to precipitant ratio of 2.7:1 at a total volume of 185 µL. Plates were incubated at 15 °C. After 24 h, CJ-LPCs have grown and are visible in solution.

HEWL Cross-linking and Trace-Labeling: After crystallization, HEWL crystals adhered to the well surface of the PYREX® spot plate. Mother liquor was removed from the crystallization well by pipette (being careful not to disturb the immobilized crystals) and replaced with 0.96 M NaCl, 50 mM sodium acetate pH 4.6 for 30 min to remove the excess HEWL monomers. The crystallization well solution was replaced with fresh 0.96 M NaCl, 50 mM sodium acetate pH 4.6, and the crystals were crosslinked for 30 min at room temperature by the direct addition of glutaraldehyde yielding a 5% (*v/v*) concentration in the crystallization well. Cross-linking reaction quench and crystal trace-labeling were achieved by replacing the crystallization well solution with 0.25 M carbohydrazide, 0.25 mM NHS-fluorescein, and 100 mM DMAB in 1x PBS pH 7.5. The HEWL crystals were removed from the surface of the PYREX® spot plate by gentle scraping and stored in fresh 4.2 M TMAO, 0.175 M H_2SO_4 at pH 7.5.

CJ-LPC Cross-linking and Trace-Labeling: After crystallization, the CJ-LPCs did not adhere to the surface of the PYREX® spot plate wells. Thus, all crystals and mother liquor in the crystallization well were transferred to a microcentrifuge tube by pipette. The CJ-LPCs remaining in the well after the initial transfer were transferred by rinsing with 4.2 M TMAO, 0.175 M H_2SO_4 pH 7.5. Crystals in solution were centrifuged on a bench top centrifuge for 2 min. The supernatant was then replaced with fresh 4.2 M TMAO, 0.175 M H_2SO_4 pH 7.5. This process was repeated twice at 10-min intervals. Light agitation was used to break up crystal pellet after the final sedimentation. Crystals were then crosslinked for 3 min at room temperature by the direct addition of glutaraldehyde or oxaldehyde at a 5% (*v/v*) final concentration. The cross-linking reaction was quenched and the crystals trace-labeled by replacing the cross-linking solution with 0.25 M carbohydrazide, 0.25 mM NHS-fluorescein, and 100 mM DMAB in 1 × PBS pH 7.5.

Citric Acid Textile Treatment: 1" x ×1" cotton fabric test swatches were placed in 2% (*w/v*) sodium borate solution for 1 h at 90 °C and subsequently rinsed with 1 × PBS pH 7.5 at room temperature. Groups of six fabric swatches were placed in 50 mL centrifuge tubes containing 25 mL 7% citric acid, 5% sodium hypophosphite, and vortexed for 1 h. Swatches were dab-dried with Kimwipes® and incubated on aluminum foil (shiny side facing swatches) in an oven at 85 °C and 160 °C for 5 min at each temperature. Citric acid-treated intermediate fabric swatches were used for further experiments within 24 h.

CDI Textile Treatment: Citric acid intermediate swatches were washed twice with new, pure acetone. Before the swatches dried, 0.25 g/mL CDI in acetone was pipetted directly onto five evenly distributed treatment locations (~12 mm diameter) on each fabric swatch and immediately sealed in an incubation apparatus with Parafilm® (Figure S1). Swatches were incubated for 3 h at room temperature and washed twice with acetone after incubation. The CDI-treated intermediate swatches were used for further experiments within 24 h.

AAD Textile Treatment: The CDI-intermediate fabric swatches were vortexed in 1 M AAD, 20 mM HEPES pH 8.0 for 3 h at room temperature and subsequently rinsed with 20 mM HEPES pH 8.0. AAD-treated intermediate swatches were used for further experiments within 24 h.

Crystal Attachment to CDI-intermediate Fabric: A total of 40 µL of crosslinked protein crystals (either variant) in 20 mM HEPES pH 8.0 were pipetted onto the treatment locations of the CDI-intermediate fabric swatches and allowed to incubate overnight at room temperature in an airtight container.

Crystal Attachment to AAD-intermediate Fabric: Protein crystals (either variant) were transferred to 20 mM HEPES pH 8.0. Glutaraldehyde (or oxaldehyde) was added to the crystal mixture to achieve a 2.5% (*v/v*) concentration in solution. After gentle mixing, the cross-linker and protein crystal solution was pipetted onto the treatment locations of the AAD-intermediate fabric swatches, placed in a sealed "sandwich" apparatus (as seen in Supplementary Figure S1), and allowed to incubate at room temperature overnight.

Crystal Retention Under Accelerated Washing: The crystal attachment retention was tested using a modified version of the colorfastness laundering protocol AATCC (American Association of Textile Chemists and Colorists) Test Method 61-2013 1A [35]. Test Method 1A (45-min duration) is meant to simulate the color change due to five careful hand-washes. Each fabric swatch containing the conjugated crystals was subjected to a 15-min accelerated laundering machine pre-wash in a steel lever-lock canister containing 200 mL DI H_2O and 10 steel beads to remove the excess non-covalently attached crystals from the fabric surface. Swatches were then washed for a total of 60 min (15-min increments) at 40 ± 2 °C in steel-lever canisters containing 200 mL DI H_2O, 0.74 g powder detergent, and 10 steel beads.

Crystal Loading: To remove the weakly adsorbed crystals, all fabric samples used for loading were subjected to a 10-min hand-shaken pre-wash in a steel lever-lock canister containing 200 mL DI H_2O and 10 steel beads. Fluorescence and differential interference contrast (DIC) imaging were conducted using a Nikon Eclipse Ti spinning-disk confocal microscope with an AndoriXon Ultra 897U EMCCD camera.

Sulforhodamine 101 Loading into HEWL Crystals: The rinsed fabric samples containing conjugated HEWL crystals labeled with NHS-fluorescein were placed in 50 mM HEPES, 150 mM NaCl, 10% glycerol pH 7.5, and imaged under brightfield light (DIC), 488 nm laser light (HEWL fluorescein), and 561 nm laser light (to test for crystal intrinsic fluorescence). After imaging, the buffer was removed and 500 µL sulforhodamine 101 (non-reactive) in 50 mM HEPES, 150 mM NaCl, 10% glycerol pH 7.5 was added directly to the fabric sample and allowed to incubate for 24 h protected from light.

Sulforhodamine-Labeled P450 Loading into CJ-LPCs: The rinsed fabric samples containing conjugated CJ-LPCs labeled with NHS-fluorescein were placed in 50 mM HEPES, 150 mM NaCl, 10% glycerol pH 7.5, and imaged under brightfield light (DIC), 488 nm laser light (CJ-LPC fluorescein), and 561 nm laser light (to test for crystal intrinsic fluorescence). After imaging, the buffer was removed and 500 µL of 50 mM HEPES, 150 mM NaCl, and 10% glycerol pH 7.5 containing cytochrome P450 labeled with sulforhodamine 101 acid chloride (NHS-TexasRed) was added directly to the fabric samples.

3. Results

3.1. Attaching the HEWL Protein Crystals to Cotton Fabric

To demonstrate the feasibility of attaching protein crystals to textiles via chemical conjugation, we first investigated the retention properties of two conjugation strategies designed to link primary amine groups on HEWL crystals to cellulose fibers within 100% cotton fabric. Small (10–100 µm diameter) tetragonal HEWL crystals were grown per a modified version of a previously described batch crystallization protocol [36]. Prior to cross-linking, crystals were washed in buffered high-salt solutions to remove residual protein monomers without compromising the integrity of the crystals. Washed crystals were then stabilized via cross-linking by the direct addition of glutaraldehyde (GA), which covalently links primary amine groups on adjacent protein monomers within the crystal scaffold. To reintroduce amines to the crystal surface, GA cross-linking intermediates were quenched with carbohydrazide. Finally, the crystals were trace labeled with NHS-fluorescein.

Fabric activation was achieved by introducing carboxylic acid groups onto the cellulose fibers within the cotton fabric using a sodium hypophosphite and citric acid (CA) treatment adapted from previous methods developed by Edwards et al. [37,38] (Figure 2A). Oxidized cotton was then incubated with 1,1′-carbonyldiimidazole (CDI) in a non-aqueous environment as detailed by Hermanson [39]; this process formed an intermediate allowing for the direct chemical attachment of amine containing substituents to the textile surface. From this CDI intermediate, short-length attachment (CDI-only) was achieved by the direct addition of protein crystals to the textile (Figure 2B). Alternatively, to form a somewhat extended molecular interface for crystal attachment, the CDI-intermediate textile was treated with adipic acid dihydrazide (AAD). Long-length attachment (CDI + AAD + GA) to the textile was therefore achieved by cross-linking the primary amine from the AAD treated textile to the protein crystal using GA (Figure 2C,D).

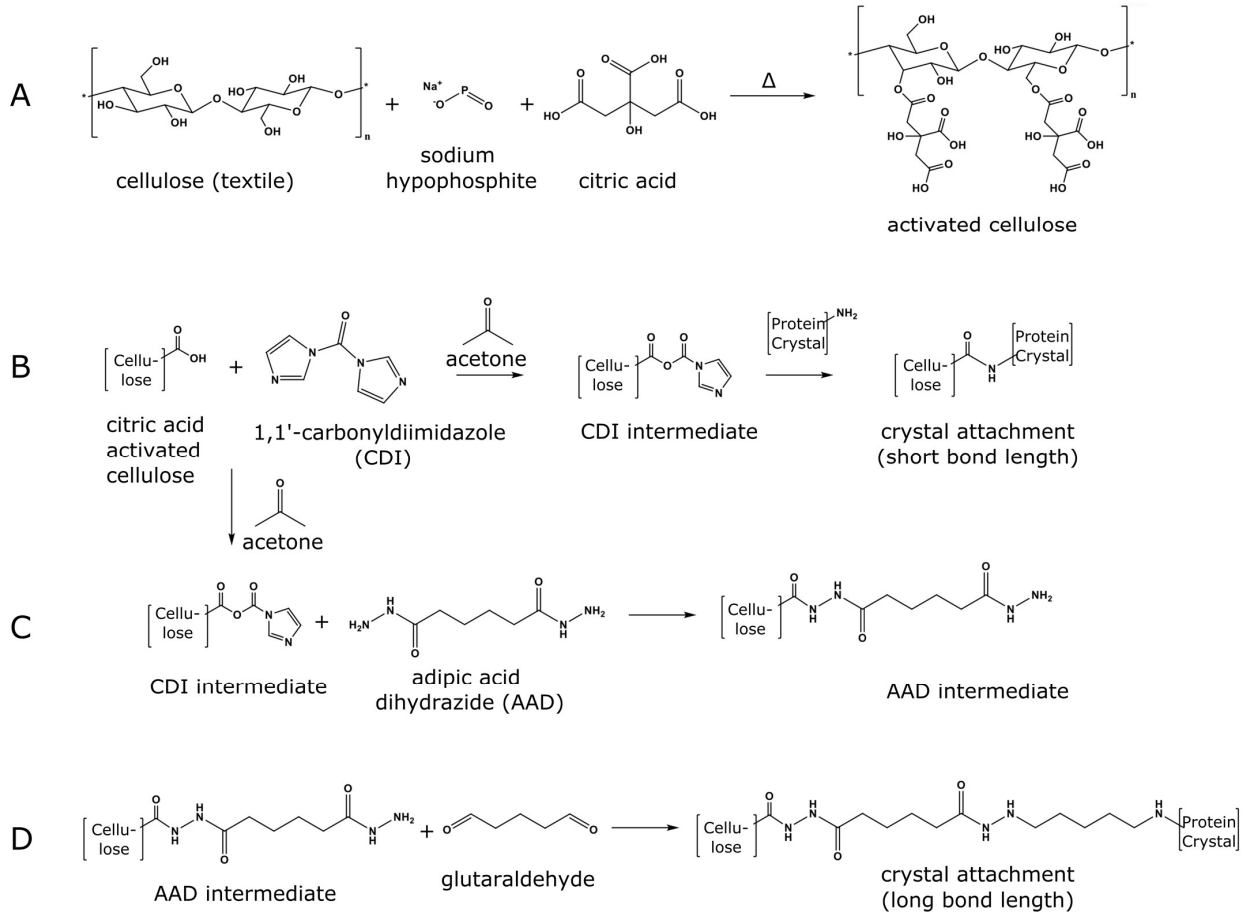

Figure 2. Protein crystal to the fabric attachment chemistries. (**A**) Formation of the surface carboxylic acid groups on the cellulose fabric (* represents the continuing polymer). (**B**) The CDI-only strategy: formation of the CDI intermediate and crystal attachment via pre-existing primary amines on the crystal surface. (**C**) The CDI + AAD + GA strategy: attachment of the AAD linker arm to the CDI intermediate followed by (**D**) crystal attachment to the AAD intermediate textile via glutaraldehyde cross-linking.

3.2. Assessing HEWL Crystal Attachment Strength

The effectiveness of the CDI-only and CDI + AAD + GA conjugation schemes was assessed using an accelerated laundering protocol based on AATCC Test Method 61 section 1A [35]. Standard 1″x ×1″ cotton test fabric swatches containing five evenly distributed areas (~12 mm diameter, Figure 3A) of attached protein crystal material were subjected to a total of 60 min of wash time in an accelerated laundering machine. HEWL crystal retention was quantified every 15 min by removing the samples and imaging them on a Typhoon FLA 7000 fluorescent scanner using an excitation wavelength of 473 nm at 10 µm resolution. Images were analyzed using the Fiji software package [40] to detect and count the fluorescent puncta corresponding to the retained trace-labeled crystals (Figure S2). See Supporting Video S2 for the CJ-LPC crystal retention on the CDI + AAD + GA treated fabric over one hour of accelerated laundering. Raw and normalized retention data are shown in Tables S1–S4.

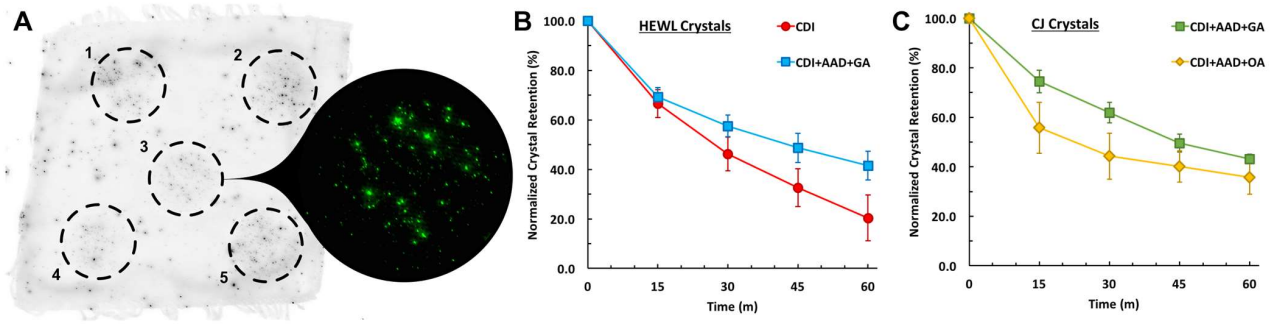

Figure 3. Results of the accelerated wash tests. (**A**) Cotton test swatch containing five areas of HEWL crystal attachment at time zero in the accelerated wash protocol. Inset: Magnified view of the center application area demonstrating the fluorescent puncta used to normalize the percent retention of protein crystals throughout the wash cycles. (**B**) Comparison of the short-length and long-length attachment reaction schemes for the HEWL crystals over 60 min of accelerated laundering time. Error Bars: standard deviation, n = 5. (**C**) Comparison of GA and OA cross-linked CJ-LPC retention over 60 min of accelerated laundering time. Error Bars: standard deviation, n = 5.

Approximately 40% of the HEWL crystals were retained on the CDI + AAD + GA treated fabric, while just over 20% of the HEWL crystals were retained on the CDI-only treated fabric after one hour of accelerated laundering. In contrast, the control swatches that were either not decorated with carboxylic acid groups or did not receive CDI showed near-zero crystal retention after rinsing in pure H_2O (Figure S3). These images revealed a substantial loss of protein crystal material in both control samples with near zero crystal retention. These results suggest that both CA activation and CDI treatment are critical for the installation of protein crystals. Similarly, CA-activated fabric treated with GA (instead of CDI) showed near-zero crystal retention (Figure S3C), indicating that the improved retention seen in the CDI + AAD + GA conjugation scheme (Figure 2C,D) is not simply due to the addition of GA alone.

We hypothesize that the increased linker arm length created by the addition of AAD and GA better overcomes the steric restrictions across the crystal-to-fabric interface, resulting in a greater number of favorable non-covalent and covalent bonds, thereby improving the overall retention. Because the CDI + AAD + GA treatment showed a marked improvement over CDI-only, the former was chosen as the preferred method for testing CJ-LPC attachment. However, it has previously been shown that oxaldehyde (OA) cross-linked CJ crystals retain diffraction better than crystals cross-linked with GA [2]. In light of this, OA cross-linked crystals and a CDI + AAD + OA conjugation strategy (identical to CDI + AAD + GA except for the substitution of OA for GA) were implemented alongside GA treatments for the CJ-LPC attachment tests.

3.3. Attaching Porous Protein Crystals to Cotton Fabric

Small (10–100 µm diameter) CJ-LPCs were grown by batch crystallization in 3.4–3.6 M $(NH_4)_2SO_4$, 40 mM bis-tris pH 6.5 at 15 °C. Crystals were cross-linked with either GA or OA, quenched with carbohydrazide, and trace labeled with NHS-fluorescein, implementing the same procedures used for tetragonal HEWL crystals. After cross-linking, crystals were conjugated to the cotton fabric either by a CDI + AAD + GA scheme or a CDI + AAD + OA scheme.

As with HEWL, approximately 40% of CJ-LPC crystals were retained on the CDI + AAD + GA treated fabric after one hour of accelerated laundering (Figure 3C). However, this retention rate dropped slightly to 35% for OA cross-linked CJ-LPC crystals on the CDI + AAD + OA treated fabric (Figure 4B). We suspect that this discrepancy is caused by GA's propensity for polymerization [41]. The polymerization of GA between the AAD primary amines and the CJ-LPC primary amines may result in longer conjugation linkages than theorized in Figure 2C. As above, we hypothesize that longer linkers allow for

more extensive bonding across the crystal-to-fabric interface when compared to a similarly structured bifunctional cross-linking agent such as OA.

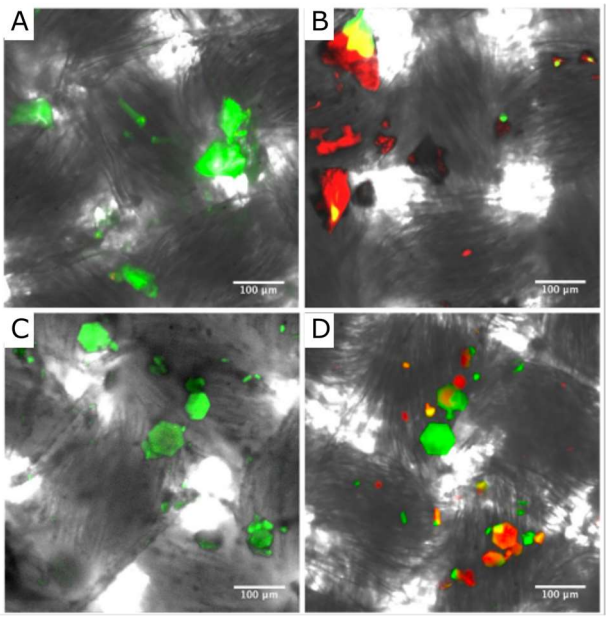

Figure 4. Composite confocal images of protein crystals conjugated to cotton fabric (DIC, 488 nm and 561 nm). (**A**) Location with empty fluorescein-labeled HEWL crystals (green). (**B**) After 24 h incubation with sulforhodamine 101, we imaged a new location showing HEWL crystals (dark gray), some with residual fluorescein signal (green), many showing sulforhodamine 101 uptake (red). (**C**) Location with empty fluorescein-labeled CJ-LPCs (green). (**D**) After 36 min incubation with sulforhodamine-labeled P450 (red), we imaged a new location showing CJ-LPCs with variable fluorescein (green) and guest enzyme (red) content. Unmerged DIC, green, and red channels are provided in Supplementary Figures S5 and S6.

3.4. Loading Guest Molecules into Textile-Attached Protein Crystals

Protein crystal conjugated cotton was loaded with guest molecules of varying sizes to demonstrate the wide range of guest functionalization. Separate fabric swatches containing either CDI + AAD + GA conjugated HEWL crystals or CDI + AAD + GA CJ crystals were first washed for 15 min in pure water to remove excess non-covalently attached crystals from the fabric surface. Cotton samples conjugated with HEWL crystals were added to 500 µL sulforhodamine 101 (Figure 1A) in a sealed vessel and incubated for 24 h protected from light. After incubation, the fabric was briefly rinsed with DI H_2O to remove the residual guest molecules. Differential interference contrast (DIC) and fluorescence (488 nm and 561 nm) confocal images showing different locations before (Figure 4A) and after (Figure 4B) incubation with sulforhodamine 101 demonstrated the HEWL crystal attachment and small molecule guest uptake. Interestingly, at the location imaged before loading (Figure 4A), there were no obvious crystals that lacked the fluorescein trace labeling, while the location imaged after loading (Figure 4B) showed a few crystal regions that had both fluorophores, many red crystals that lacked fluorescein, some green crystals that lacked sulforhodamine 101, and some crystals that lacked both (dark gray). The component DIC image, green emission and red emission channels for the post-loading sample location are shown in Supplementary Figure S5.

Similarly, the CJ-LPC conjugated fabric was soaked in 500 µL of sulforhodamine-labeled cytochrome P450 heme domain to demonstrate the potential for enzyme loading. The cytochrome P450 heme domain used as a model guest enzyme was a synthetic homolog to the soluble P450s of *Bacillus megaterium* and *Bacillus subtilis* [42]. Specifically, we used

a purified aliquot of chimera 21311331, where each numeral indicates the parent enzyme (1: CYP102A1 (Figure 1B), 2: CYP102A2, 3: CYP102A3).

After the addition of P450, images were taken on a confocal/fluorescence microscope at 488 nm and 561 nm every 2 min for 36 min (see Figure S4 and Supplementary Video S2). Throughout a time-lapse video of guest loading, anisotropic diffusion of the P450 enzyme into the CJ-LPC pores was observed (Supplementary Video S3, Supplementary Figure S4). Afterward, DIC and fluorescence (488 nm and 561 nm) z-stack confocal images were taken, demonstrating macromolecular guest uptake (Figure 4D) via comparison with a comparable location imaged prior to loading (Figure 4C). The component DIC image, green emission and red emission channels for the post-loading sample location are shown in Supplementary Figure S6. Notably, this study only demonstrated the enzyme loading and did not extend to studying the enzyme release nor intra-crystal activity. However, Kowalski et al. demonstrated activity for two enzymes (glucose oxidase and horseradish peroxidase) inside the CJ crystals that were crosslinked with oxaldehyde [43].

Neither fluorescent labeling nor non-covalent loading achieved 100% labeling or uptake. To prepare a conservative estimate for the fraction of CJ crystals that took up the fluorescent guest enzyme, we conducted a frame-by-frame analysis of the post-incubation z-stack provided by Supplementary Video S3. Approximately 33% of the distinct CJ crystals (35/106) had sufficient uptake of the red fluorescent guest enzyme to visibly differ from the empty crystals (green). In contrast, most of the HEWL crystals were able to uptake sulforhodamine 101 (the saturated red crystals visible in Figure 4A, right). Some HEWL crystals (dark grey domains) lacked both the green and red fluorophores. Despite the imperfect yield, these results indicate that a range of guest molecules can be loaded into different porous protein crystal scaffolds that have been conjugated to cellulose fibers in cotton textiles.

4. Discussion

The myriad topologies of protein crystals provide a wide range of pore structures and dimensions. As such, these materials can accommodate adsorbates of varying size, from small molecules to macromolecular guests. Here, we demonstrated that versatile guest molecule storage materials may be created from inexpensive cotton fabrics functionalized by conjugated protein crystals. There was a clear separation of timescales in the guest retention between the bare textile and the protein crystal reservoirs, with reservoirs achieving superior retention. Furthermore, the loading times required for each guest molecule depend on the host crystal. By rationally selecting the host crystal pore structure, one could conceivably optimize the storage or transport kinetics of guest molecules based on the size, charge, or hydrophobicity. Furthermore, multi-species guest loading and release may be possible by conjugating a variety of protein crystal reservoirs, each optimized for a specific guest molecule. Alternately, a sufficiently modular porous crystal platform could be engineered to include affinity domains for tuning the cargo capacity or release kinetics.

This method of loading guest molecules into the void space of protein crystals conjugated to textiles may prove a reliable method for the extended, metered release of a variety of molecules. We have previously demonstrated guest molecule release in response to changes in pH [31,33]; thus, it may be feasible to trigger the release of guest molecules from textile bound protein crystal reservoirs using environmental cues such as pH or exposure to analytes. Characterizing guest loading and release kinetics under varying environmental conditions may be an attractive follow-up study. Applications of this technology range from medical wound dressings to multifunctional textiles exhibiting anti-microbial and anti-malarial properties. Future practitioners who test this conjugation strategy should determine whether the chemical treatment of the cotton impacts the properties of the material. For example, citric acid activation may cause cellulose hydrolysis [44].

5. Conclusions

The current pioneering study demonstrates that robust crystal attachment to cotton is possible, but leaves significant room for improvement. Accelerated laundering for 60 min always resulted in the loss of at least half of the initially attached crystals. While further optimization of the covalent conjugation chemistry strategy may improve crystal retention, careful crystal size selection and improved physical placement of the crystals on the fabric might also improve retention. This study also demonstrated that small molecule cargo (sulforhodamine 101) and large molecule cargo (a model enzyme) can be loaded into the HEWL and CJ crystals, respectively, that were previously attached to cotton. However, there is again room for improvement since the majority of the CJ crystals did not take up guest cargo. It is possible that the crystal nanopores collapsed or became blocked during crystal washing, crosslinking, or conjugation. Ideally, a follow-on study will determine at which step some crystals lost the ability to uptake guest molecules. Notably, the degree to which the crosslinked protein lattices retained crystalline precision after washing was not characterized here. Future studies should quantify both the guest binding capacity and the extent to which the host matrix preserves hallmarks of crystallinity such as birefringence and diffraction.

Supplementary Materials: The following supporting information can be downloaded at: https://www.mdpi.com/article/10.3390/cryst13020352/s1, Figure S1: CDI treatment apparatus; Figure S2: Representative Typhoon image and puncta detection; Table S1: HEWL crystal retention using CDI-only conjugation; Table S2: HEWL crystal retention using CDI + AAD + GA conjugation; Table S3: CJ-LPC crystal retention using CDI + AAD + OA conjugation; Table S4: CJ-LPC crystal retention using CDI + AAD + GA conjugation; Figure S3: Crystal attachment controls; Figure S4: Guest enzyme loading time-lapse; Video S1: CrystalRetentionLaunderingCycles.avi; Video S2: PorousCrystalEnzymeLoading.avi; Video S3: EnzymeLoadedZStack.avi.

Author Contributions: Conceptualization, C.D.S.; Methodology, L.F.H.; Software, L.F.H.; Validation, L.F.H., L.P.G., and L.B.J.; Investigation, L.F.H., D.A.A., L.P.G., and L.B.J.; Resources, Y.V.L.; Data curation, L.F.H.; Writing—original draft preparation, L.F.H. and L.P.G.; Writing—review and editing, L.F.H., D.A.A., and C.D.S.; Supervision, L.F.H. and C.D.S.; Project administration, C.D.S.; Funding acquisition, C.D.S. All authors have read and agreed to the published version of the manuscript.

Funding: This material is based upon work supported by the National Science Foundation under grant no. 1506219.

Institutional Review Board Statement: Not applicable.

Informed Consent Statement: Not applicable.

Data Availability Statement: All data generated are provided in the Supplementary Materials.

Acknowledgments: This specific project was initiated with support from the Natick Soldier Research Development and Engineering Center. The authors thank the following NSRDEC members for the materials and helpful discussions: Shaun Filocamo, June Lum, Shalli Sherman, and Laura Place.

Conflicts of Interest: The authors declare no conflict of interest.

References

1. Tabe, H.; Shimoi, T.; Boudes, M.; Abe, S.; Coulibaly, F.; Kitagawa, S.; Mori, H.; Ueno, T. Photoactivatable CO release from engineered protein crystals to modulate NF-κB activation. *Chem. Commun.* **2016**, *52*, 4545–4548. [CrossRef] [PubMed]
2. Hartje, L.F.; Bui, H.T.; Andales, D.A.; James, S.P.; Huber, T.R.; Snow, C.D. Characterizing the Cytocompatibility of Various Cross-Linking Chemistries for the Production of Biostable Large-Pore Protein Crystal Materials. *ACS Biomater. Sci. Eng.* **2018**, *4*, 826–831. [CrossRef] [PubMed]
3. Noritomi, H.; Koyama, K.; Kato, S.; Nagahama, K. Increased Thermostability of Cross-Linked Enzyme Crystals of Subtilisin in Organic Solvents. *Biotechnol. Tech.* **1998**, *12*, 467–469. [CrossRef]
4. Sobolov, S.B.; Bartoszko-Malik, A.; Oeschger, T.R.; Montelbano, M.M. Cross-linked enzyme crystals of fructose diphosphate aldolase: Development as a biocatalyst for synthesis. *Tetrahedron Lett.* **1994**, *35*, 7751–7754. [CrossRef]
5. Sobolov, S.B.; Leonida, M.D.; Bartoszko-Malik, A.; Voivodov, K.I.; McKinney, F.; Kim, J.; Fry, A.J. Cross-Linked LDH Crystals for Lactate Synthesis Coupled to Electroenzymatic Regeneration of NADH. *J. Org. Chem.* **1996**, *61*, 2125–2128. [CrossRef]

6. Khalaf, N.; Govardhan, C.P.; Lalonde, J.J.; Persichetti, R.A.; Wang, Y.-F.; Margolin, A.L. Cross-Linked Enzyme Crystals as Highly Active Catalysts in Organic Solvents. *J. Am. Chem. Soc.* **1996**, *118*, 5494–5495. [CrossRef]
7. Xu, K.; Klibanov, A.M. pH Control of the Catalytic Activity of Cross-Linked Enzyme Crystals in Organic Solvents. *J. Am. Chem. Soc.* **1996**, *118*, 9815–9819. [CrossRef]
8. Wang, Y.-F.; Yakovlevsky, K.; Zhang, B.; Margolin, A.L. Cross-Linked Crystals of Subtilisin: Versatile Catalyst for Organic Synthesis. *J. Org. Chem.* **1997**, *62*, 3488–3495. [CrossRef]
9. Visuri, K.; Pastinen, O.; Wu, X.; Mäkinen, K.; Leisola, M. Stability of native and cross-linked crystalline glucose isomerase. *Biotechnol. Bioeng.* **1999**, *64*, 377–380. [CrossRef]
10. St. Clair, N.; Wang, Y.-F.; Margolin, A.L. Cofactor-Bound Cross-Linked Enzyme Crystals (CLEC) of Alcohol Dehydrogenase. *Angew. Chem. Int. Ed.* **2000**, *39*, 380–383. [CrossRef]
11. Roy, J.J.; Abraham, T.E. Continuous biotransformation of pyrogallol to purpurogallin using cross-linked enzyme crystals of laccase as catalyst in a packed-bed reactor. *J. Chem. Technol. Biotechnol.* **2006**, *81*, 1836–1839. [CrossRef]
12. Lopez, S.; Rondot, L.; Leprêtre, C.; Marchi-Delapierre, C.; Ménage, S.; Cavazza, C. Cross-Linked Artificial Enzyme Crystals as Heterogeneous Catalysts for Oxidation Reactions. *J. Am. Chem. Soc.* **2017**, *139*, 17994–18002. [CrossRef] [PubMed]
13. Vilenchik, L.Z.; Griffith, J.P.; St. Clair, N.; Navia, M.A.; Margolin, A.L. Protein Crystals as Novel Microporous Materials. *J. Am. Chem. Soc.* **1998**, *120*, 4290–4294. [CrossRef]
14. Pastinen, O.; Visuri, K.; Leisola, M. Xylitol purification by cross-linked glucose isomerase crystals. *Biotechnol. Tech.* **1998**, *12*, 557–560. [CrossRef]
15. Pastinen, O.; Jokela, J.; Eerikäinen, T.; Schwabe, T.; Leisola, M. Cross-linked glucose isomerase crystals as a liquid chromatographic separation material. *Enzyme Microb. Technol.* **2000**, *26*, 550–558. [CrossRef]
16. Leisola, M.; Jokela, J.; Finell, J.; Pastinen, O. Simultaneous catalysis and product separation by cross-linked enzyme crystals. *Biotechnol. Bioeng.* **2001**, *72*, 501–505. [CrossRef]
17. Vuolanto, A.; Kiviharju, K.; Nevanen, T.K.; Leisola, M.; Jokela, J. Development of Cross-Linked Antibody Fab Fragment Crystals for Enantioselective Separation of a Drug Enantiomer. *Cryst. Growth Des.* **2003**, *3*, 777–782. [CrossRef]
18. Vuolanto, A.; Leisola, M.; Jokela, J. Enantioselective Affinity Chromatography of a Chiral Drug by Crystalline and Carrier-Bound Antibody Fab Fragment. *Biotechnol. Prog.* **2004**, *20*, 771–776. [CrossRef]
19. Basu, S.K.; Govardhan, C.P.; Jung, C.W.; Margolin, A.L. Protein crystals for the delivery of biopharmaceuticals. *Expert Opin. Biol. Ther.* **2004**, *4*, 301–317. [CrossRef]
20. Puhl, S.; Li, L.; Meinel, L.; Germershaus, O. Controlled Protein Delivery from Electrospun Non-Wovens: Novel Combination of Protein Crystals and a Biodegradable Release Matrix. *Mol. Pharm.* **2014**, *11*, 2372–2380. [CrossRef]
21. Tabe, H.; Shimoi, T.; Fujita, K.; Abe, S.; Ijiri, H.; Tsujimoto, M.; Kuchimaru, T.; Kizaka-Kondo, S.; Mori, H.; Kitagawa, S.; et al. Design of a CO-releasing Extracellular Scaffold Using in Vivo Protein Crystals. *Chem. Lett.* **2014**, *44*, 342–344. [CrossRef]
22. Tabe, H.; Fujita, K.; Abe, S.; Tsujimoto, M.; Kuchimaru, T.; Kizaka-Kondoh, S.; Takano, M.; Kitagawa, S.; Ueno, T. Preparation of a Cross-Linked Porous Protein Crystal Containing Ru Carbonyl Complexes as a CO-Releasing Extracellular Scaffold. *Inorg. Chem.* **2015**, *54*, 215–220. [CrossRef]
23. Luiz de Mattos, I.; Lukachova, L.V.; Gorton, L.; Laurell, T.; Karyakin, A.A. Evaluation of glucose biosensors based on Prussian Blue and lyophilised, crystalline and cross-linked glucose oxidases (CLEC(R)). *Talanta* **2001**, *54*, 963–974. [CrossRef]
24. Roy, J.J.; Abraham, T.E.; Abhijith, K.S.; Kumar, P.V.S.; Thakur, M.S. Biosensor for the determination of phenols based on cross-linked enzyme crystals (CLEC) of laccase. *Biosens. Bioelectron.* **2005**, *21*, 206–211. [CrossRef] [PubMed]
25. Laothanachareon, T.; Champreda, V.; Sritongkham, P.; Somasundrum, M.; Surareungchai, W. Cross-linked enzyme crystals of organophosphate hydrolase for electrochemical detection of organophosphorus compounds. *World J. Microbiol. Biotechnol.* **2008**, *24*, 3049–3055. [CrossRef]
26. Conejero-Muriel, M.; Rodríguez-Ruiz, I.; Verdugo-Escamilla, C.; Llobera, A.; Gavira, J.A. Continuous Sensing Photonic Lab-on-a-Chip Platform Based on Cross-Linked Enzyme Crystals. *Anal. Chem.* **2016**, *88*, 11919–11923. [CrossRef]
27. Matthews, B.W. Solvent content of protein crystals. *J. Mol. Biol.* **1968**, *33*, 491–497. [CrossRef] [PubMed]
28. Cvetkovic, A.; Straathof, A.J.J.; Hanlon, D.N.; van der Zwaag, S.; Krishna, R.; van der Wielen, L.A.M. Quantifying anisotropic solute transport in protein crystals using 3-D laser scanning confocal microscopy visualization. *Biotechnol. Bioeng.* **2004**, *86*, 389–398. [CrossRef] [PubMed]
29. Cvetkovic, A.; Picioreanu, C.; Straathof, A.J.J.; Krishna, R.; van der Wielen, L.A.M. Quantification of binary diffusion in protein crystals. *J. Phys. Chem. B* **2005**, *109*, 10561–10566. [CrossRef]
30. Cvetkovic, A.; Picioreanu, C.; Straathof, A.J.J.; Krishna, R.; Wielen, L.A.M. Relation between pore sizes of protein crystals and anisotropic solute diffusivities. *J. Am. Chem. Soc.* **2005**, *127*, 875–879. [CrossRef] [PubMed]
31. Kowalski, A.E.; Huber, T.R.; Ni, T.W.; Hartje, L.F.; Appel, K.L.; Yost, J.W.; Ackerson, C.J.; Snow, C.D. Gold nanoparticle capture within protein crystal scaffolds. *Nanoscale* **2016**, *8*, 12693–12696. [CrossRef]
32. Hartje, L.F.; Munsky, B.; Ni, T.W.; Ackerson, C.J.; Snow, C.D. Adsorption-Coupled Diffusion of Gold Nanoclusters within a Large-Pore Protein Crystal Scaffold. *J. Phys. Chem. B* **2017**, *121*, 7652–7659. [CrossRef]
33. Huber Thaddaus, R.; Hartje Luke, F.; McPherson Eli, C.; Kowalski Ann, E.; Snow Christopher, D. Programmed Assembly of Host–Guest Protein Crystals. *Small* **2017**, *13*, 1602703. [CrossRef] [PubMed]

34. Huber, T.R.; McPherson, E.C.; Keating, C.E.; Snow, C.D. Installing Guest Molecules at Specific Sites within Scaffold Protein Crystals. *Bioconjug. Chem.* **2018**, *29*, 17–22. [CrossRef] [PubMed]
35. AATCC Test Method (61-2013), Color Fastness to Laundering: Accelerated, Technical Manual Method American Association of Textile Chemists and Colorists. 2017; 108.
36. Hekmat, D.; Hebel, D.; Schmid, H.; Weuster-Botz, D. Crystallization of lysozyme: From vapor diffusion experiments to batch crystallization in agitated ml-scale vessels. *Process Biochem.* **2007**, *42*, 1649–1654. [CrossRef]
37. Vincent Edwards, J.; Prevost, N.; Condon, B.; Sethumadhavan, K.; Ullah, J. Immobilization of Lysozyme on Cotton Fabrics: Synthesis, Characterization, and Activity. *AATCC Rev.* **2011**, *11*, 73–79.
38. Edwards, J.V.; Prevost, N.T.; Condon, B.; French, A. Covalent attachment of lysozyme to cotton/cellulose materials: Protein verses solid support activation. *Cellulose* **2011**, *18*, 1239–1249. [CrossRef]
39. Hermanson, G.T. *Bioconjugate Techniques*, 3rd ed.; Elsevier/AP: London, UK; Waltham, MA, USA, 2013; ISBN 978-0-12-382239-0.
40. Schindelin, J.; Arganda-Carreras, I.; Frise, E.; Kaynig, V.; Longair, M.; Pietzsch, T.; Preibisch, S.; Rueden, C.; Saalfeld, S.; Schmid, B.; et al. Fiji: An open-source platform for biological-image analysis. *Nat. Methods* **2012**, *9*, 676–682. [CrossRef]
41. Migneault, I.; Dartiguenave, C.; Bertrand, M.J.; Waldron, K.C. Glutaraldehyde: Behavior in aqueous solution, reaction with proteins, and application to enzyme crosslinking. *BioTechniques* **2004**, *37*, 790–796, 798–802. [CrossRef]
42. Otey, C.R.; Landwehr, M.; Endelman, J.B.; Hiraga, K.; Bloom, J.D.; Arnold, F.H. Structure-guided recombination creates an artificial family of cytochromes P450. *PLoS Biol.* **2006**, *4*, e112. [CrossRef]
43. Kowalski, A.E.; Johnson, L.B.; Dierl, H.K.; Park, S.; Huber, T.R.; Snow, C.D. Porous protein crystals as scaffolds for enzyme immobilization. *Biomater. Sci.* **2019**, *7*, 1898–1904. [CrossRef] [PubMed]
44. Bondancia, T.J.; de Aguiar, J.; Batista, G.; Cruz, A.J.G.; Marconcini, J.M.; Mattoso, L.H.C.; Farinas, C.S. Production of Nanocellulose Using Citric Acid in a Biorefinery Concept: Effect of the Hydrolysis Reaction Time and Techno-Economic Analysis. *Ind. Eng. Chem. Res.* **2020**, *59*, 11505–11516. [CrossRef]